Preliminary Design Exploration of Prospective Multirotor Aerobots for Mars

Vishal Youhanna[1], Leonard Felicetti[1], Dmitry Ignatyev[1]

[1]School of Aerospace, Transport and Manufacturing, Cranfield University, Cranfield, UK

Abstract

The groundbreaking success of NASA's Ingenuity Helicopter has spurred immense potential for Martian exploration, emphasizing the pivotal role of aerobots alongside rovers and landers. However, the helicopter's limitations, stemming from its compact and simplistic design, are apparent in its restricted long-range endurance and payload capacity. This paper suggests a feasible optimisation approach for Martian rotorcraft concepts while addressing constraints and progressing Martian drone technology. The key focus lies in improving performance to meet the evolving demands of forthcoming Martian aerobot missions. Based on a comprehensive parametric analysis rooted in simplified rotorcraft momentum theory, this study focuses on power requirements of rotorcrafts with single, coaxial, tandem, quad and hexa rotors for hover, vertical climb, and forward flight segments. Modified to meet more demanding mission criteria, these designs are limited by the spacecraft aeroshell's maximum size for safe transport to Mars. Among the considered configurations, the hexacopter emerged as the most efficient choice, offering a balance between performance, endurance, and payload capacity, while a conventional single main rotor configuration fell short within the specified parameters.

Keywords: Martian Aerial Drones, Planetary UAV, Rotorcraft Conceptual Design

1. Introduction

1.1 Planet Mars

The increasing interest in Mars exploration has catalysed the development of specialised aerial robots, known as aerobots, to support the sustainability of future missions in Mars' thin atmosphere. Prior to 2021, Mars missions primarily utilised spacecraft, landers, and rovers. However, unmanned aerial vehicles have gained attention for their advantages over surface rovers, including greater speed, wider range, superior obstacle avoidance, and enhanced visibility [1]. Historically, planetary exploration favoured lighter-than-air airships or fixed-wing planes due to the technical complexities of rotor-based aerobots. Nevertheless, recent advancements in drone technology have renewed interest in rotorcraft for Mars exploration.

Mars' unique atmospheric conditions present significant challenges for rotorcraft design. Although Mars has lower gravity, its atmospheric density is approximately 100 times lower than Earth's [2], resulting in very low Reynolds numbers for rotor operations, particularly for small-scale helicopters. However, the Mach number on Mars would be significantly higher due to two main factors: the necessity for higher tip speeds to compensate for the lower atmospheric density, and the reduced speed of sound on the Martian surface, which is only about 72% of that on Earth. These conditions impose substantial design constraints on rotorcraft [3]. A crucial challenge in sustaining flight for Martian drones is managing the heat generated by the propulsion system while generating the necessary lifting thrust, especially given the low Reynolds numbers. Furthermore, the use of an aeroshell with a maximum diameter of 4.5 m for aerobot transport to Mars introduces additional complexities [4]. Historically, these elements have raised questions about the practicality of using rotorcraft on Mars. However, NASA's accomplishment in April 2021 with the deployment of the Ingenuity Mars Helicopter has discredited such scepticism.

Published by ICAS. © The Author. Issued with the Creative Commons Attribution Licence (CC BY 4.0).
Please refer to any applicable publisher terms of use.
https://www.icas.org/ICAS_ARCHIVE/ICAS2024/data/preview/ICAS2024_0536.htm

1.2 Literature

Ingenuity, before retiring in February 2024, completed 72 short autonomous pre-commanded flights [5]. These flight tests transitioned Ingenuity from the Technology Demonstration phase to the Operations Demonstration phase, highlighting the potential for collaboration between future rovers and aerial surveyors. The knowledge gained from designing and operating the Mars Helicopter provides valuable insights for developing advanced aerobots for Mars exploration. Despite Ingenuity's success, its small size and basic configuration limit its endurance, range, and payload capacity, hindering its ability to conduct comprehensive scientific missions requiring long-distance flights, larger scientific payloads, advanced communication systems, or robust propulsion systems for high-altitude missions.

To address these limitations, this paper proposes enhancing the design of aerobots by setting more ambitious requirements for Martian aerobot missions. This involves developing a new rotorcraft design while considering practical operational and design constraints, including adhering to a maximum aeroshell diameter of 4.5 m, assuming that launch and re-entry technologies will remain relatively stable in the coming decades. The South-West (SW) Melas Basin of Melas Chasma within the Valles Marineris canyon system on Mars is selected as the mission location. Despite its rugged terrain presenting challenges, advancements in navigational planetary landing technology and the obstacle avoidance capabilities of aerobots make this site a promising candidate for in-situ exploration [3]. An aerobot deployed in this region could produce high-resolution aerial maps and identify potential locations for experimental sample collection for future rover missions. The primary mission objective is to capture high-quality images of the surveyed areas and effectively transmit this visual data to a rover from the same mission or a ground control station on Earth.

Increasing the size or adding fixed wings to the Ingenuity Helicopter is one way to enhance its capabilities. Vertical takeoff and landing (VTOL) fixed-wing aircraft with both rigid and retractable body configurations have been investigated in several Mars mission plans [6]-[11]. Young et al. (2000) introduced the pioneering concept of rotary VTOL planetary aerial vehicles, exemplified by the Mars tiltrotor, which balances hover performance and cruise range, crucial for Mars exploration [6]. Various innovative designs, such as the Y-4 Tilt-Rotor VTOL Aerobot [7] and MIRAGE [8], utilise different propulsion configurations, including tiltrotors, coaxial rotors, and embedded fans. Concepts like tailsitters [9] and hopper [10] designs offer alternative approaches for Mars exploration, with projects like VALKERIE merging inflatable wing technology for transport efficiency [11]. NASA's second-generation Mars helicopters [4], including the Mars Science Helicopter (MSH) and Advanced Mars Helicopter (AMH), feature foldable designs with varying rotor sizes and payloads.

1.3 Proposed Study

Meeting more demanding specifications requires the development of new rotorcraft designs that adhere to practical limitations, particularly the maximum aeroshell diameter. It may be necessary to package a large rotorcraft with a smaller ground spacecraft, transport it separately, or use an innovative folding mechanism within the aeroshell to accommodate it. A comprehensive parametric analysis of rotorcraft designs is necessary to determine the overall benefits of larger or winged Martian rotorcraft and propose suitable configurations for further research. In a recent study by the authors [12], performance analysis of various battery-electric rotorcraft configurations with single, dual, and quad rotors was conducted within defined parameters, including initial sizing estimation. This paper extends the analysis by incorporating hexacopter configuration and improved adjustments to the parameters used, broadening the scope of investigation to encompass a wider range of design possibilities and performance outcomes.

The research article outlines a generalised methodology (section 2) based on simplified momentum theory for calculating the flight power of various Martian rotorcraft configurations, including those with overlapping rotors. Additionally, a method for initial sizing of battery-electric aircraft (section 3) estimates required battery mass based on flight power, aiding in determining the total rotorcraft mass. Study cases for parametric analysis (section 4) are established, involving single conventional helicopters, coaxial rotorcraft, three tandem rotorcraft configurations, quadcopter and hexacopter

configuration. Then all the parameters are defined and summarised (section 5). Results and analysis (section 6) focus on power demands for hover, vertical climb, and forward flight across these configurations, informing the identification of the most power-efficient designs. However, theoretical optima may introduce complexities due to design constraints, necessitating careful configuration selection and refinement, as discussed in the penultimate section 7.

2. POWER REQUIREMENT ANALYSIS METHODOLOGY FOR ROTORCRAFT

2.1 Rotorcraft Types

Figure 1 depicts six rotorcraft configurations, including single, dual, quad, and hexarotor. Traditional rotary-wing aircraft usually have a single main rotor on top of the fuselage that provides both lift and thrust, along with a tail rotor to counteract torque. Coaxial rotorcraft, which have two rotors on the same axis rotating in opposite directions, do not require a tail rotor and are inherently more stable. Tandem rotor designs feature two main rotors placed one behind the other along the fuselage, which increases lift capacity and payload potential. Side-by-side rotorcraft include configurations such as tiltrotors and tiltwings, with multiple rotors positioned closely together, allowing for flexible operation in both hovering and forward flight. Quadcopters, a subtype of multicopters, have a four-rotor arrangement known for its simplicity, stability, and ease of control, making them a popular choice for UAVs and drones used on Earth. Hexacopters, with six rotors, offer enhanced stability and payload capacity compared to quadcopters, making them suitable for more demanding applications requiring greater lift and redundancy.

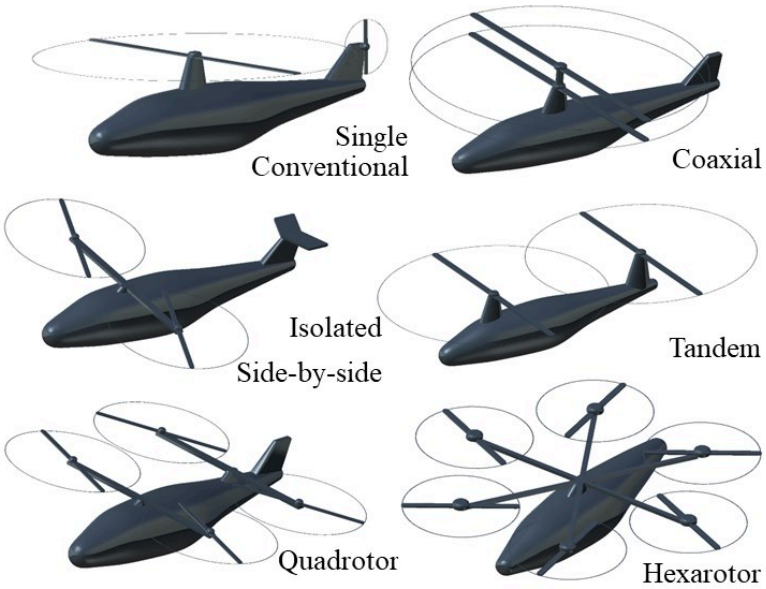

Figure 1 Rotorcraft Configurations Illustration

2.2 Conventional Rotorcraft

The key factor determining the success of a reusable Martian aerobot is its ability to perform vertical takeoff and landing (VTOL), given that Mars lacks conventional runways. This VTOL capability is entirely dependent on the efficiency of its rotor propulsion system. To estimate the power consumption of the rotor during different flight phases such as hovering, vertical climb, and forward flight, momentum theory is applied. In this model, the rotor blades are treated as actuator disks with negligible thickness and a specific disk area (S). The model assumes uniform airflow distribution across the rotor disk and immediate energy transfer to the airflow, while disregarding factors like airfoil profile drag losses, tip losses, and residual rotational velocities. To address these omissions, the figure of merit concept is introduced. This figure of merit (M) is the ratio of ideal power to actual power ($M = P_{ideal} / P_{actual}$) and indicates rotor efficiency. Equation (1) provides the calculation for the power required for vertical climb or hover (when climb velocity is zero), specifically for a conventional helicopter [13]. The total power required also factors in the energy needed for the tail rotor. Typically, the power ratio of the tail rotor to the main rotor ($P_{\text{tail rotor}}/P_{\text{main rotor}}$) ranges from 0.14 to 0.22, as tail rotors generally have a diameter that is about 15-20% of the main rotor's diameter [13].

$$P_{(\text{Vert Climb or Hover})} = \left[\left(\frac{fW}{M}\sqrt{\frac{fW/S}{2\rho}}\right) + \frac{WV_{\text{Climb}}}{2}\right]\left[\frac{(1 + P_{\text{tail rotor}}/P_{\text{main rotor}})}{\eta_{\text{mechanical}}}\right], \quad (1)$$

where $P\ (\text{Watt})$ is the power required; $W\ (N)$ is the rotorcraft weight (=mg, where $m\ (\text{kg})$ is the mass of the rotorcraft and $g\ (m/s^2)$ is the surface gravity acceleration on Mars for the sake of this paper); $S\ (m)$ is the rotor disk area; M is the figure of merit; $V_{\text{Climb}}\ (m/s)$ is vertical climb velocity (=0 for hover); f is the adjustment for downwash on the fuselage (=1.06 typically); $\rho\ (\text{kg}/m^3)$ is the local air density on Mars; $\eta_{\text{mechanical}}$ is mechanical losses adjustment due to driving of the tail rotor (=0.97 typically)

During forward flight, the rotor acts like a circular wing with an aspect ratio of $4/\pi$. Empirical data indicates an Oswald efficiency factor for such wings between 0.5 and 0.8 [13]. This factor, determined at a given lift coefficient, is the ratio of the induced drag coefficient of the wing to that of an elliptical wing with the same aspect ratio at the same lift coefficient. Parasitic drag is expressed in terms of drag area (D/q), where 'q' is the dynamic pressure. The following equation integrates these elements, helps estimate the power needed for forward climb or level flight [13].

$$P_{(\text{Fwd}_{\text{climb}} \text{ or } \text{Fwd}_{\text{level}})} = \left[\frac{V}{\eta_p}\left\{q(D/q) + \frac{W^2}{4eqS} + W\sin(\gamma)\right\}\right]\left[\frac{(1+P_{\text{tail rotor}}/P_{\text{main rotor}})}{\eta_{\text{mechanical}}}\right], \quad (2)$$

where $V\ (m/s)$ is the forward flight speed; $\gamma\ (\text{Deg})$ is the climb path angle (=0, when levelled); $q\ (\text{Pa})$ is the dynamic pressure; e is the equivalent Oswald's efficiency factor (=0.5 to 0.8 typically); $D/q\ (m^2)$ is the component drag area; η_p is the propeller efficiency (=0.6 to 0.85 typically).

In the equation, $W\sin(\gamma)$ represents the climb component, which depends on the climb path angle γ (equal to 0 for level flight). The rotor not only provides the necessary lift but also generates forward propulsion, functioning similarly to a propeller. Therefore, the propeller efficiency factor η_p is included in the calculation to provide a more accurate estimate of the rotor's forward thrust performance.

2.3 Coaxial Rotorcraft

In the traditional helicopter setup, the tail rotor serves to counteract the torque created by the main rotor's rotation by generating an opposing thrust. Another method to manage this torque involves substituting the tail rotor with an additional rotor of the same size but rotating in the opposite direction, thus providing extra lift. This method is exemplified in coaxial rotorcraft, where two rotors are mounted on the same shaft within a complex hub structure. However, the proximity of these rotors results in some loss of lift due to interference from the airflow wake. Theoretically, when the two rotors perfectly overlap, with zero vertical gap, the overlapping interference factor (K_{ov}) increases power consumption by approximately $\sqrt{2}$ or around 41% compared to two isolated rotors unaffected by the wake of each other [14]. When there is no vertical separation between the rotors in a coaxial setup, it is termed an equivalent single rotor system. This equivalent single rotor resembles a system of smaller twin rotors with the same total thrust and projected area (disk loading), sharing similar rotor solidity [15]. Disk loading is the ratio of the helicopter's total weight to the rotor disk area (W/S), while rotor solidity is the ratio of total blade area to total disk area.

In practical scenarios, coaxial rotor configurations typically has some vertical separation between the two rotors. As this separation increases, the upper rotor's wake affects a smaller portion of the lower rotor, leading to a reduction in the overlapping interference factor (K_{ov}). For example, with a large separation (LS), typically around 10% of the rotor diameter, the K_{ov} becomes 1.281, assuming uniform disk loading [14] [15]. Consequently, Eq. (1), used to compute the power required for vertical climb and hover for a coaxial rotor system with two equally sized rotors sharing the total rotorcraft weight (thrust), is adjusted by multiplying it by the overlapping interference factor to form Eq. (3). Similarly, Eq. (2), used for the forward flight of a conventional helicopter, is adapted to form Eq. (4) for a coaxial helicopter [14].

$$P_{(\text{Vert Climb or Hover})} = \left[\left(\frac{fW}{(2\sqrt{2})M}\sqrt{\frac{fW/S}{2\rho}}\right) + \frac{WV_{\text{Climb}}}{4}\right]\left[\frac{2}{\eta_{\text{mechanical}}}\right][K_{ov}] \quad (3)$$

$$P_{(\text{Fwd}_{\text{climb}} \text{ or } \text{Fwd}_{\text{level}})} = \left[\frac{V}{\eta_p}\left\{q(D/q) + \frac{W^2}{16eqS} + \frac{W\sin(\gamma)}{2}\right\}\right]\left[\frac{2}{\eta_{\text{mechanical}}}\right][K_{ov}] \quad (4)$$

In this setup, there's no tail rotor; instead, a second rotor is employed. As a result, the power ratio between the two equal-sized rotors ($P_{\text{second rotor}}/P_{\text{main rotor}}$) becomes equal to 1.

2.4 Isolated Rotors: rotorcraft having non-overlapping rotors

The K_{ov} factor, representing the degree of overlapping interference between equally sized rotors, transitions from $\sqrt{2}$ to 1 as their shared area moves from complete overlap to complete absence within the same plane. When there is no overlap, these rotors essentially operate independently. However, residual interference, whether advantageous or detrimental, might still be present in cases of vertical rotor separation without overlap, although it can be disregarded in preliminary investigations [14] [15]. One variant of side-by-side rotor configurations is transverse rotorcraft, such as tiltrotors and tiltwings, where smaller rotors are horizontally mounted on the tips of side wings or an extended support frame of the fuselage. These smaller rotors are usually positioned to avoid overlap and function more like separate rotors. During cruise flight, they serve as forward propellers. In situations involving configurations of multiple rotors without overlap, like quad or hexa rotors, equations (1) and (2) can be adapted to accommodate a multirotor system with ' N ' equally sized rotors. In such arrangements, the total thrust needed for the rotorcraft is assumed to be evenly distributed among all the rotors, as outlined in equations (5) and (6).

$$P_{(\text{Vert Climb or Hover})} = \left[\left(\frac{fW}{(N\sqrt{N})M}\sqrt{\frac{fW/S}{2\rho}}\right) + \frac{WV_{\text{Climb}}}{2N}\right]\left[\frac{N}{\eta_{\text{mechanical}}}\right] \quad (5)$$

$$P_{(\text{Fwd}_{\text{climb}} \text{ or } \text{Fwd}_{\text{level}})} = \left[\frac{V}{\eta_p}\left\{q(D/q) + \frac{W^2}{(N^2)4eqS} + \frac{W\sin(\gamma)}{N}\right\}\right]\left[\frac{N}{\eta_{\text{mechanical}}}\right] \quad (6)$$

In configurations where rotors are aligned front-to-rear, an additional downwash effect is generated by the front rotor onto the rear one(s) in the forward flight. To ensure accurate power estimation, this downwash influence must be factored into the calculations for the rear rotor(s) [14], as detailed in the subsequent section on tandem configurations. The revised equation substitutes [N] with $[1 + (P_{\text{tail rotor}}/P_{\text{main rotor}})]$ to indicate the number of rotors involved. This adjustment recognizes that in such configuration, there is no tail rotor; instead, all rotors are of equal size.

2.5 Rotorcraft with Partial Overlapping Rotors (e.g., Tandem Rotorcraft)

In tandem rotorcraft setups, two equal-sized rotors are arranged longitudinally on the fuselage, with one rotor positioned ahead of the other. The analysis of this configuration mirrors that of coaxial rotors, with overlapping disk areas determined by the horizontal gap between the rotors. Maximum tandem overlap occurs when one rotor's blade tip touches the hub center of the other rotor. Therefore, the initial power analysis of vertical climb or hover for tandem rotors follows the same formula as that used for coaxial rotors, as described in Eq. (3). However, in a tandem configuration, the calculation of the overlapping interference factor (K_{ov}) is affected by the ratio (d/D), representing the horizontal distance (d) between the two rotor axes to the rotor diameter (D). When the rotors are in the same plane (i.e., no vertical gap between rotors), K_{ov} can be approximated using Eq. (7) [14].

$$K_{ov} = \left[\sqrt{2} - \frac{\sqrt{2}}{2}\left(\frac{d}{D}\right) + \left(1 - \frac{\sqrt{2}}{2}\right)\left(\frac{d}{D}\right)^2\right] \quad (7)$$

When rotors are positioned in separate planes and the lower rotor operates within the contracting wake of the upper rotor, determining the overlapping area for K_{ov} calculation requires numerical integration. Moreover, side-by-side rotor configurations with overlapping rotors can adopt a similar approach to assess overall power requirements.

In estimating the power needed for forward flight in tandem rotorcraft, it is crucial to consider the downwash effect on the rear rotor caused by the presence of the front rotor. This downwash must be quantified and integrated into the calculation to accurately determine power loss. For initial theoretical analysis, this downwash (dw) is assumed to be the maximum value of the overlapping interference factor (max $\mathrm{K_{ov}}$ = $\mathrm{K_{dw}}$) [14], which is 1.134 when calculated using Eq. (7) at maximum tandem overlap. Hence, the total power (P) required for forward flight is expressed by Eq. (8) [14]. In this preliminary analysis, it is assumed that the two equal-sized rotors generate equal thrust, thus requiring equal power consumption. Therefore, this expression is represented in Eq. (9), where the total power for forward flight of two isolated rotors (calculated using Eq. (6)) is divided by two and then multiplied by the downwash factor. Additionally, if there is an overlap between the two rotors, the overlapping interference factor $(\mathrm{K_{ov}})$ is incorporated into the expression to calculate the total forward power.

$$\mathrm{P_{(Forward)}} = \mathrm{P_{Front\ Rotor}} + \mathrm{P_{Rear\ Rotor}}(\mathrm{K_{dw}})\,, \tag{8}$$

$$\mathrm{P_{(Forward)}} = (1 + \mathrm{K_{dw}})\frac{1}{2}\mathrm{P_{2\ Iso}}\mathrm{K_{ov}}\,, \tag{9}$$

where $\mathrm{P_{2\ Iso}}$ (Watt) is the required forward flight power of rotorcraft with 2 isolated rotors; K_{dw} is the downwash factor (=1.134); K_{ov} is the overlapping interference factor (=1, when no overlapping).

In scenarios without rotor overlap, such as non-overlapping same-plane tandem rotor configurations, the inclusion of $\mathrm{K_{ov}}$ is either omitted or its value is set to 1 in equations (3) and (9). This adjustment is crucial since the use of Eq. (7) for estimating $\mathrm{K_{ov}}$ becomes inaccurate when there is no rotor overlap.

3. Initial Sizing Methods for Battery-Electric Aircraft

Initial sizing of battery-electric aircraft involves accounting for the total mass of the aircraft at maximum take-off, including the empty mass, payload, and fuel components. In fuel-powered aircraft, mass decreases during flight due to fuel consumption across various flight stages: taxiing, take-off, ascent, cruising, and descent. This mass reduction affects aircraft performance and drag characteristics, necessitating detailed calculations for each flight phase during initial sizing evaluations. In contrast, electric aircraft do not experience variations in battery mass during flight, eliminating the need for integration across flight segments. Instead, the fuel component of total aircraft mass is replaced with the mass of the battery (m_b). The required battery mass for each mission segment is determined using Eq. (10), which expresses it as a ratio of the battery mass to the total aircraft mass (m_b/m_0), known as the Battery Mass Fraction (BMF) [13].

$$\mathrm{BMF} = \frac{m_\mathrm{b}}{m_0} = \frac{\mathrm{W_b}}{\mathrm{W_0}} = \frac{\mathrm{EP_{used}}}{\mathrm{E_{sb}}\eta_{\mathrm{b2s}} m_0}\,, \tag{10}$$

where m_0 (kg) is the total take-off mass of the aerobot; m_b (kg) is the battery mass; $\mathrm{W_0}$ (N) is the total take-off weight of the aerobot (=mg, where g $(\mathrm{m/s^2})$ is the surface gravity acceleration on Mars for this paper); $\mathrm{W_b}$ (N) is the battery weight; $\mathrm{P_{used}}$ $(\mathrm{Watt\ or\ W})$ is the power required; E $(\mathrm{hour\ or\ h})$ is the known run time; $\mathrm{E_{sb}}$ $(\mathrm{Wh/kg})$ is the battery-specific energy; η_{b2s} is the total system efficiency from the battery to the motor output shaft (=0.9 typically).

The equation above considers parameters such as the known run-time endurance (E) and the power consumption during various flight phases, including vertical climb, hover, and forward flight for rotorcraft. The cumulative Battery Mass Fraction (BMF) of the aircraft is then calculated by summing the BMFs corresponding to each flight phase [13]. This methodology enables a comprehensive assessment of the battery mass required for different stages of the aircraft's mission. Equation (11) is utilised to determine the total aircraft take-off mass (m_0), which is defined as the sum of the empty mass, battery mass, and payload mass [13].

$$m_0 = m_\mathrm{e} + m_\mathrm{b} + m_\mathrm{payload} \tag{11}$$

Eq. (11) undergoes modification to formulate Eq. (12) for battery electric aircraft sizing [13].

$$m_0 = \frac{m_{\text{payload}}}{1 - \text{BMF}_{\text{total}} - \frac{m_e}{m_0}} \quad (12)$$

This adjustment involves considering both the total Battery Mass Fraction and the ratio of empty mass (m_e) to total mass [13]. In this context, the payload may consist of instruments or items for delivery, particularly for unmanned aircraft. Conversely, m_e encompasses all components except the payload or operational batteries, including the propulsion system, aircraft structure, avionics, navigation equipment, and other essential systems.

The initial sizing equation provides a starting point for preliminary estimations, taking into account factors such as the empty mass ratio, payload mass, and the calculated BMF requirement. These parameters allow for the determination of the total mass. Alternatively, known parameters can be utilised to infer unknown variables, such as estimating total mass and empty mass, and subsequently calculating the required BMF to assess the payload capacity of the aircraft. This sizing procedure involves iteration and may require multiple computations and adjustments until a reasonable estimate aligns with the desired objectives, facilitating preliminary design investigations.

4. Definition of Rotorcraft Configurations

4.1 Tandem Rotorcraft Cases

The arrangement of tandem rotorcraft can vary depending on how the rotors are longitudinally positioned on the fuselage. Considering the structural constraints of the aeroshell, three scenarios are examined for the analysis of power consumption (also detailed in [16]). In these scenarios, the two equal-sized rotors are placed at equidistant points from the midpoint, resulting in displacements of 2.25 m, 1.125 m, and 0.75 m for Cases 1, 2, and 3, respectively. This assumes that the fuselage length matches the maximum size of the aeroshell, which is 4.5 m. Figure 2 illustrates these rotor positions on the aerobot fuselage within an aeroshell dome. These configurations represent extreme scenarios for parametric analysis (Figure 3): Case 1 positions foldable rotors at the fuselage ends, allowing for a maximum diameter of 9 m; Case 3 situates the rotors to fit within the aeroshell boundary, with a maximum diameter of 3 m; and Case 2 falls in between, enabling rotors with a maximum diameter of 4.5 m. It is important to note that, in practical applications, rotor blades must be spaced from the inner walls of the aeroshell and rotor hubs. However, this theoretical study does not consider such clearances.

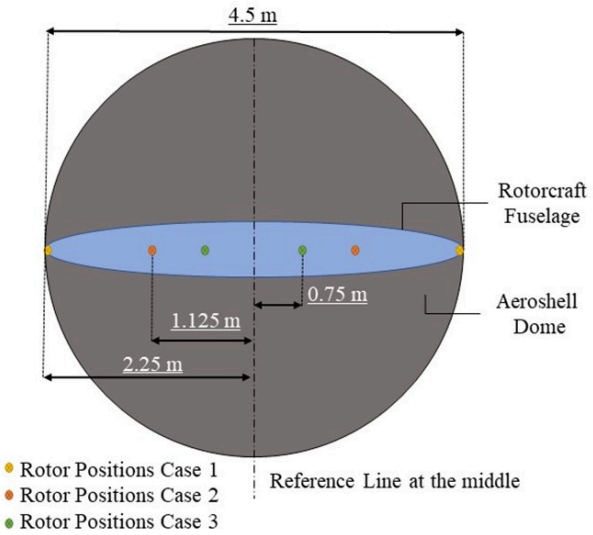

Figure 2 Schema of the positioning of rotor hubs of tandem rotorcraft Cases 1, 2, and 3, on the fuselage placed inside an aeroshell [16]. (Not to scale)

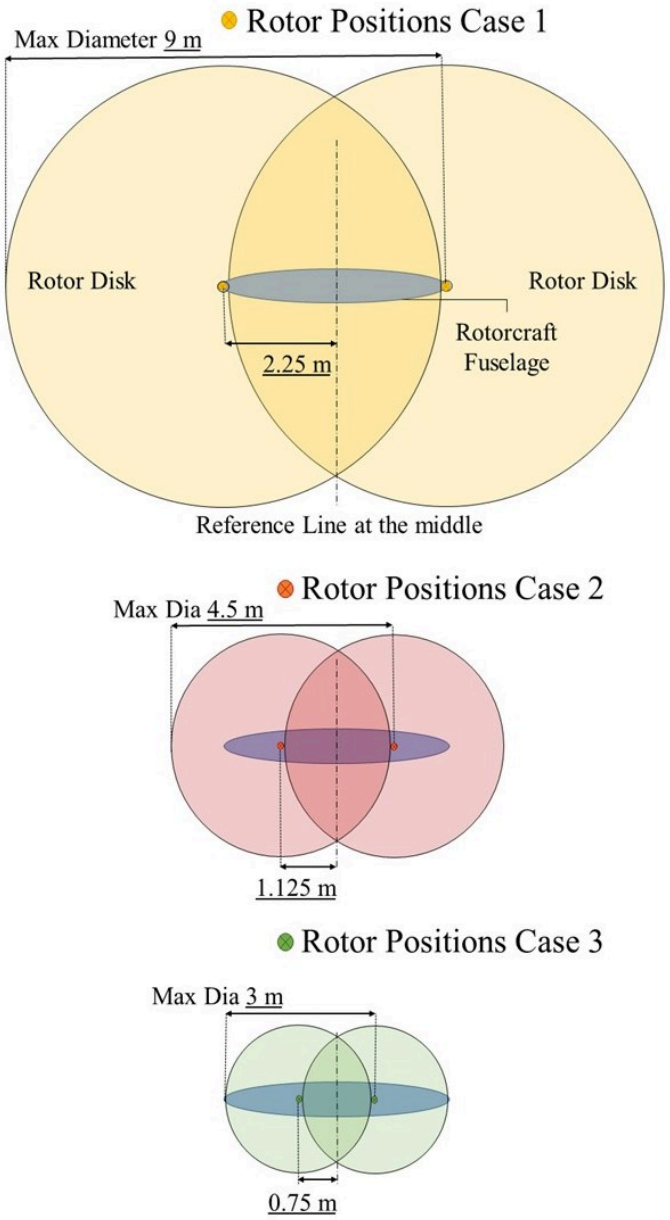

Figure 3 Diagrammatic illustration of the rotor positioning of tandem rotorcraft Cases 1, 2, and 3 in operational mode [12]. (Not to scale)

In Case 1, a folding mechanism, potentially with an articulated rotor hub system, are needed to fit within the aeroshell for storage if the rotor diameter exceeds 2.25 m. Similarly, Case 2 would require identical folding mechanisms and possibly an articulated rotor hub system if the rotor diameter surpasses 2.25 m. In contrast, Case 3 permits the use of a rigid rotor hub system without the need for linkages. An outline of the defined parameters for each of the three tandem rotorcraft cases is provided in Table 1, along with quadcopter case and hexacopter case (to be discussed subsequently).

4.2 Quadcopter and Hexacopter Cases

Both quadcopter and hexacopter configurations can vary depending on the longitudinal placement of the rotor hub support frames atop the fuselage, similar to the tandem rotorcraft configuration cases mentioned earlier. However, such multicopters typically feature non-overlapping rotors, and therefore, only such a layout is considered in this study. A quadcopter configuration is established for parametric analysis, where two non-overlapping, equal-sized rotors are positioned at 1.125 m from the midpoint on each side. Figure 4 visually depicts the defined parameters for the quadcopter case (also detailed in [12]). Similarly, hexacopter configuration is established for parametric analysis, where six non-overlapping, equal-sized rotors are positioned at a radial distance of 1.5 m from the centre with 60° apart from each other. Figure 5 visually depicts the defined parameters for the hexacopter case.

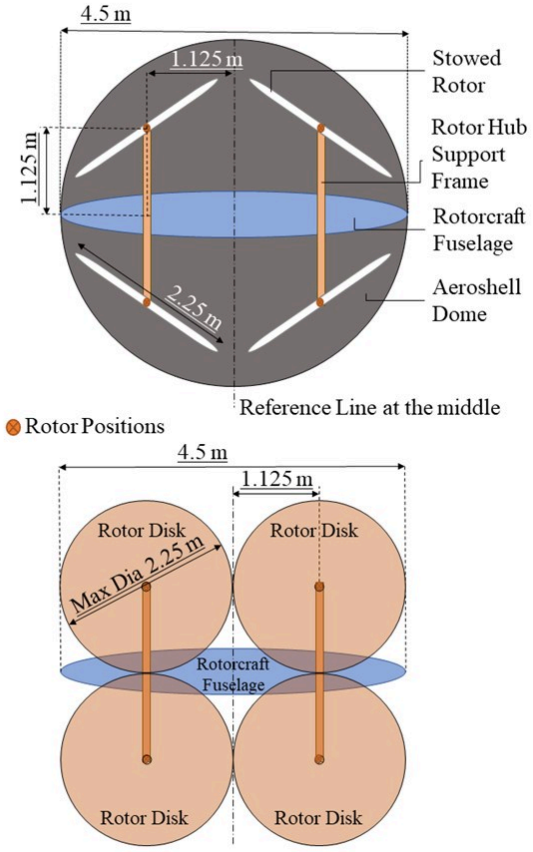

Figure 4 Diagram (not to scale) of the rotor hub positioning of quadrotor configuration with nonoverlapping equal-sized rotors. Top - stowed inside aeroshell. Bottom - operational mode [12]

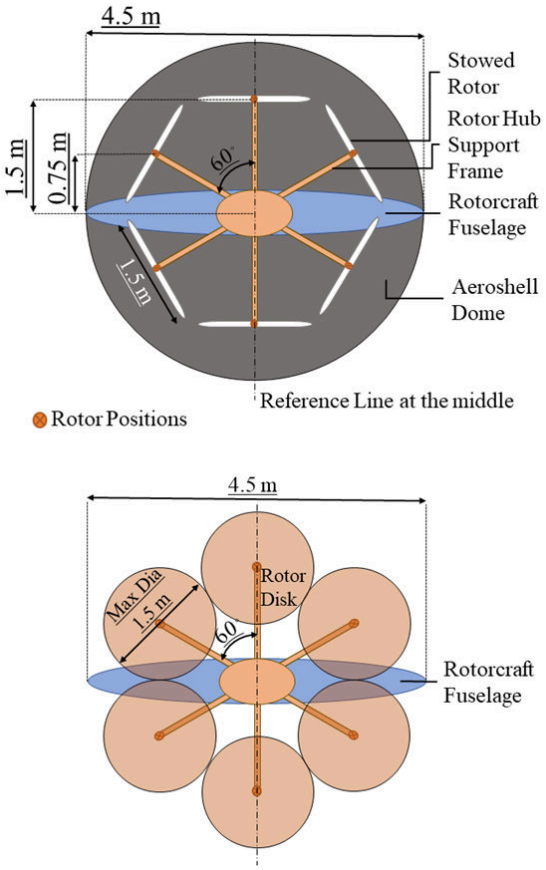

Figure 5 Schematic illustration (not to scale) of the rotor hub positioning of hexarotor configuration with nonoverlapping equal-sized rotors. Top - stowed inside aeroshell. Bottom - operational mode

The established quadcopter and hexacopter configurations ensure a maximum allowable rotor diameter without overlap during operation or stowage inside the aeroshell dome. The rotor diameter is limited to 2.25 m to prevent overlapping for quadrotor and 1.5 m for hexarotor. These configurations can utilise a rigid rotor hub system. Detailed information is provided in Table 1.

Table 1 Summary of Tandem Quad & Hexa Rotorcraft Cases

Case No.	Rotor System Type	Folding Mechanism	Maximum Diameter	Rotor Position*	Isolated Rotor behaviour
Tandem 1	Articulated	Yes	9 m	2.25 m	D ≤ 4.5 m
Tandem 2	Articulated**	Yes**	4.5 m	1.125 m	D ≤ 2.25 m
Tandem 3	Rigid	No	3 m	0.75 m	D ≤ 1.5 m
Quad	Rigid	No	1.25	1.125 m	D ≤ 2.25 m
Hexa	Rigid	No	1.5	1.5 m***	D ≤ 1.5 m

* Rotor hub position from the center of the fuselage

** When rotor D is > 2.25 m

***Radial position from the centre

5. Definition of Parameters for Performance Analysis

During rotorcraft flight, the encountered air density is a crucial factor for initial power sizing considerations. Mars' average surface air density is approximately 0.02 kg/m³ [17], although it varies based on location, altitude relative to sea level, and changes with seasons and time of day. For the primary mission in SW Melas Chasma, approximately 2 km below the datum, the Mars Climate Database (Version 6.1) [18] is utilised to estimate regional air density values during a flight time corresponding to the 11th hour of local solar time [19]. This investigation yielded a mean air density estimate of 0.016 kg/m³. The maximum allowable size of the aerobot is limited by the diameter and height of the protective aeroshell, set at 4.5 m and approximately 2.2 m, respectively, constraining the design and evaluation of Martian aerobot configurations. The rotor disk size range considered for the parametric performance study of design configurations spans from 5% to 100% (i.e., 0.23m to 4.5m) of the aeroshell diameter, apart from tandem rotorcraft case 1 which goes up to 9m diameter.

On Mars, operational restrictions are imposed on rotor tip speed and forward velocity to prevent the formation of transonic compression waves, given the sound speed of approximately 240 m/s (Ref. 3). Typically, rotor advancing blade tip speed is limited to about 0.75 Mach (180 m/s), ensuring adequate lift sustenance on the retreating blade during forward flight, requiring the advancing blade's speed to be nearly three times that of a helicopter [13]. Consequently, a maximum forward speed of 60 m/s is advised, equivalent to one-third of the maximum rotor tip speed and one-quarter of Mars' average sound speed. Rotorcraft sizing is based on range, cruising speed, takeoff, and ascent, and assumes continuous high-power operation. Descent and landing phases are omitted for simplicity [13]. The flight profile in this study (depicted in Figure 6) entails a 2-minute ascent to 1 km (at an average vertical climb velocity of 8.33 m/s), followed by a 3-minute traverse of 10 km (with an average cruising velocity of 55.56 m/s), culminating in vertical descent. This theoretical method's outcomes align well with experimental data when the aircraft's advance ratio ranges from 0.1 to 0.3 [14]. The advance ratio of a rotorcraft denotes the ratio of its forward flight speed to its rotor tip speed.

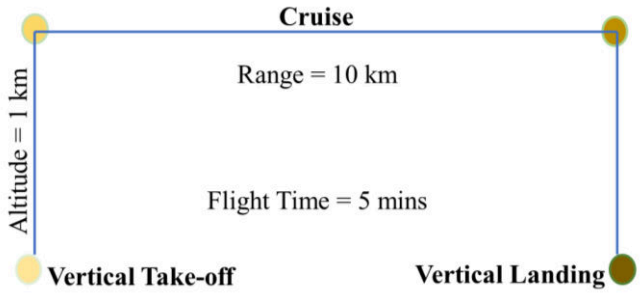

Figure 6 Flight profile for the performance analysis

Table 2 summarises the parameters discussed in this subsection that are utilised in the power analysis

for various rotorcraft configurations during forward flight, vertical climb, and hover phases. For the mission, the aerobot's Maximum Take-Off Gross (MTOG) mass is fixed at 20 kg. An average value of 0.6 for the figure of merit, M, is employed, considering its typical range from 0.6 to 0.8 [13]. Additionally, based on a JPL technological projection, the battery's specific energy (E_{sb}), which is utilised to calculate the Battery Mass Fraction (BMF) for flights, is anticipated to be 230 Wh/kg [4].

Table 2 Parameters utilised in analysing power requirements for forward flight, vertical climb, and hover across various rotorcraft configurations.

Parameter		**Values**		**Unit**
Mars Mean Air Density at SW Melas Basin		0.016		kg/m^3
Speed of Sound		240		m/s
Surface Gravity Acceleration on Mars		3.73		m/s^2
Aircraft MTOG Mass		20		kg
Aircraft MTOG Weight, W		74.60		N
Allowable Max Rotor Advancing Tip Mach Number, M_{at}		0.75		Mach
Air Speed at Max M_{at} on Mars		180		m/s
Traverse Range as per Flight Mission		10		km
Cruise Flight Endurance, E		3.0		min
Cruise Flight Velocity, V		55.56		m/s
Dynamic Pressure at the Cruise Velocity, q		24.69		Pa
Flight Altitude as per Flight Mission		1		km
Vertical Climb Endurance, E		2.00		min
Average Vertical Climb Velocity,V_{climb}		8.33		m/s
Rotor Blade Diameter, Blade D	0.23	to	9.0	m
Rotor Disk Area, S	0.04	to	63.6	m^2
Battery Specific Energy, E_{sb}		230.00		Wh/kg
Figure of Merit, M		0.6		
Mechanical efficiency factor, $\eta_{mechanical}$		0.97		
Fuselage downwash adjustment, f		1.06		
Helicopter Power ratio ($P_{tail\ rotor}/P_{rotor}$)		0.18		
Coaxial Power ratio ($P_{second\ rotor}/P_{main\ rotor}$)		1		
System efficiency battery to motor (η_{b2s})		0.9		
Propeller Efficicency, η_p		0.8		
Oswald Efficiency, e		0.5		
Parasitic Drag Area, D/q (Front Area x Drag data)	**Front Area**	**Drag Data**	**D/q**	
D/q Fuselage (radius 0.15 m)	7.1E-02	0.09	6.0E-03	m^2
D/q Tubular Landing 4 legs (0.002m x 0.03m, each)	2.4E-04	1.01	2.4E-04	m^2
D/q Unfaired Single Rotor Hub (0.005m x 0.003m)	1.5E-05	1.20	1.8E-05	m^2
Downwash Interference Drag Fuselage	7.1E-02	0.02	1.4E-03	m^2
Leakage & Protuberance Drag (15% Total D/q)			1.2E-03	m^2

There are a few other parameters that are essential for forward flight analysis, including the frontal area of the aircraft body. The fuselage's frontal size, landing legs, and unfaired rotor hub remain consistent across all variants. Helicopter-specific drag statistics published by D. Raymer [13] provide the drag area (D/q) per unit frontal area, which can be multiplied by the helicopter's frontal area to derive specific values for each component's drag area. The calculated total parasitic drag is then integrated into the conventional helicopter's Eq. (2) and, correspondingly, into the forward flight equations for other type of rotorcrafts. While drag data may not precisely determine parasitic drag, it serves adequately for initial sizing of rotorcraft until the design progresses sufficiently for further exploratory research.

6. Results and Analysis

6.1 Hover and Vertical Climb Analysis

In Figure 7, the power required for a conventional Martian helicopter is plotted against the rotor disk diameter. As the rotor diameter increases, so does the rotor disk area, leading to a decrease in disk

loading (W/S, total weight divided by disk area). Lower disk loading implies less battery power is needed for hovering or ascending, allowing for a higher power loading (W/P) - which represents the ratio of the helicopter's weight to its engine power. However, it is crucial to acknowledge that reduced disk loading results in larger rotor blades, contributing to increased weight, higher drag during forward flight, and a heightened risk of encountering shocks on the advancing blade [13], aspects not covered in this study.

The graph indicates that smaller rotors consume significantly more power than larger ones, with power decreasing noticeably and dramatically as rotor disk diameter increases (also discussed in [12] and [16], however different values of parameters such as figure of merit (M), fuselage downwash (f) and Oswald's efficiency factor (e) are used in this whole analysis for better estimation). Additionally, as the aerobot's total mass increases, the power required for smaller rotor disks rises sharply, while the increase in power demand for larger rotor disk diameters is minimal. This disparity is evident in the 40 kg versus 20 kg Helicopter graph shown in Figure 7. It is apparent from the power requirements that the helicopter requires slightly more power for vertical ascent than for hovering, which is expected due to the energy needed for vertical forward propulsion. However, over time, the difference between the two power requirements becomes more pronounced as the rotor disk size increases.

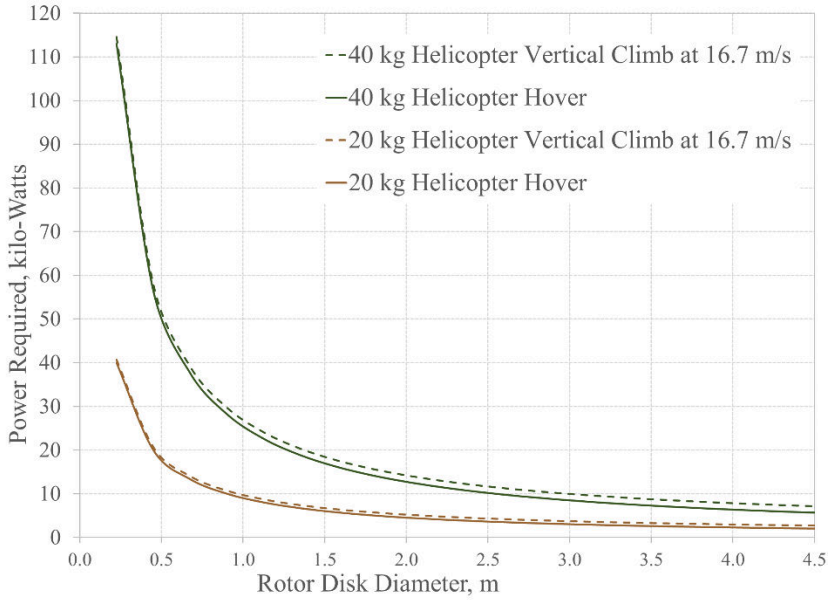

Figure 7 Power Required vs Rotor Disk Diameter - 20 kg & 40 kg Martian Conventional Helicopter

The graph plots in Figure 8 and Figure 9 illustrate the hover power and vertical climb power (at a velocity of 8.33 m/s) respectively, across various rotorcraft designs relative to the rotor disk diameter. These configurations encompass the conventional helicopter, LS (large separation) coaxial rotorcraft, three tandem rotorcraft cases, rotorcraft with two isolated rotors, quadcopter and hexacopter cases. While the inclusion of power data for two isolated rotors is primarily for analytical comparison with tandem rotor Case 1, it serves to highlight significant trends. Corresponding to the pattern observed in the helicopter power requirements graph, all configurations exhibit higher power demands for vertical climbing compared to hovering, with this disparity increasing as the rotor disk diameter grows. Among these, the conventional helicopter stands out for consuming the most power.

In contrast, the power consumption of two equal-sized coaxial rotors is notably lower, especially with smaller rotor sizes. For instance, at a rotor size of 0.23 m in diameter, the coaxial rotorcraft consumes roughly 9000 Watts less power, while tandem rotorcraft configurations require about 16,000 Watts less power than the conventional helicopter for both hovering and vertical climbing. Similarly, the quadrotor requires approximately 23,000 Watts less power, whereas hexacopter require around 26000 Watts lesser power. At the maximum aeroshell size (corresponding to a rotor diameter of 4.5 m), hover and vertical climb power requirements remain below 2,500 Watts for all configurations.

Interestingly, across all three tandem rotorcraft scenarios, the power consumption of the tandem rotorcraft system aligns with that of the two isolated rotors before any overlap occurs between them. Furthermore, the power requirements for all variants decrease inversely and stabilize as the rotor

diameter increases. As seen in tandem rotorcraft Case 1, this difference becomes negligible for rotor disk sizes between 4.5 and 9 m. Noteworthy is the significantly lower power consumption of quadcopter and hexacopter compared to all other rotorcraft types, particularly when employing smaller rotor diameters.

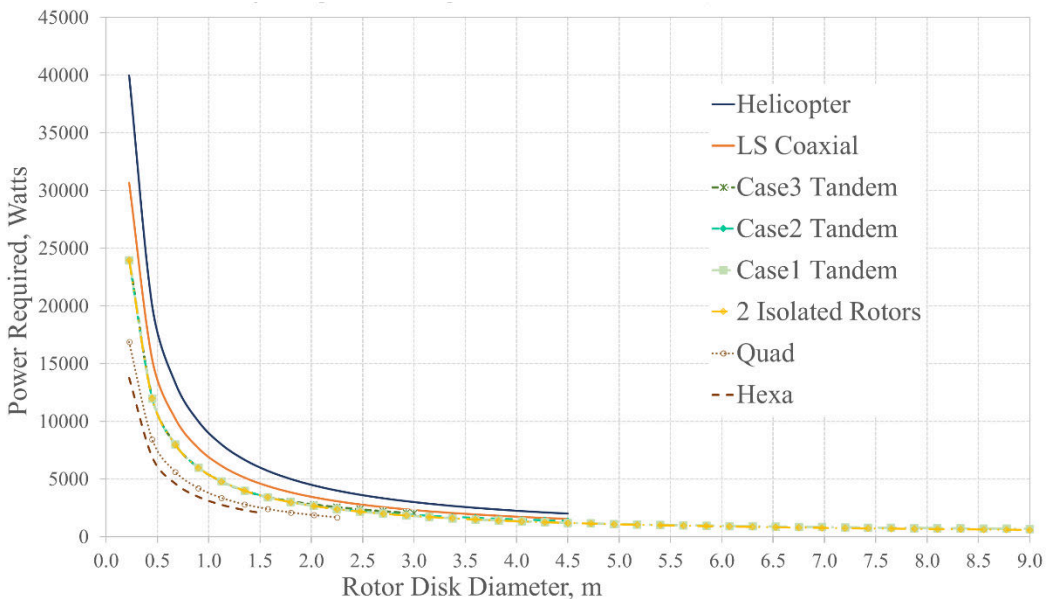

Figure 8. Hover Power Required vs Rotor Disk Diameter – Comparison between various 20 kg rotorcraft configurations (Helicopter, Coaxial, Tandem Cases, 2 Isolated Rotors, Quadcopter, Hexacopter)

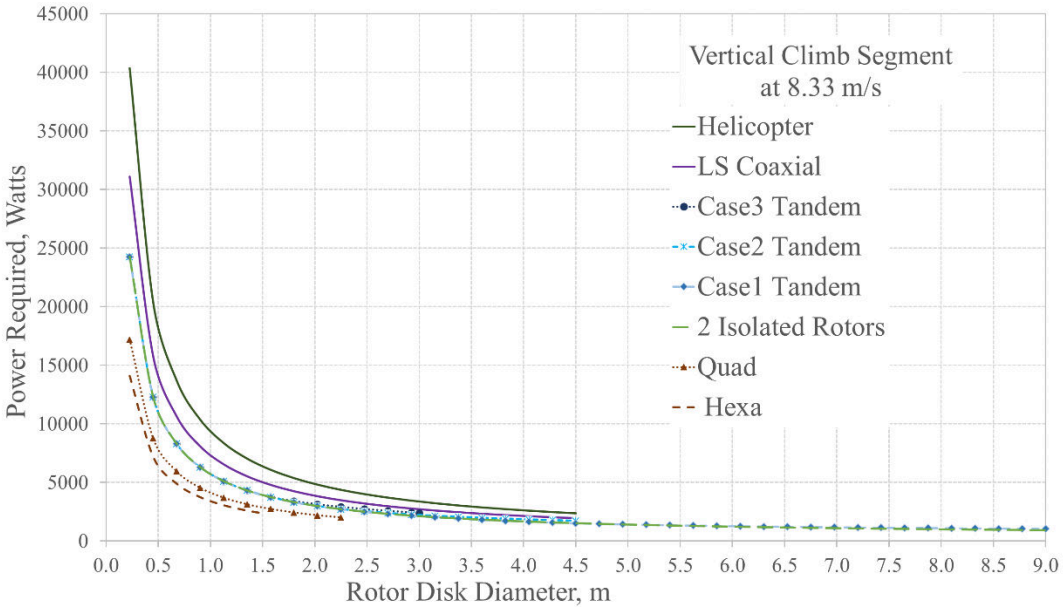

Figure 9. Vertical Climb Power Required (at 8.33 m/s) vs Rotor Disk Diameter – Comparison between various 20 kg rotorcraft configurations (Helicopter, Coaxial, Tandem Cases, 2 Isolated Rotors, Quadcopter, Hexacopter)

6.2 Forward Flight Analysis

The power required for forward leveled flight and forward climb flight at a 20-degree climb path angle is analyzed for each of the specified rotorcraft configurations, considering a forward flying speed of 55.56 m/s. Figure 10 illustrates the power required for a Martian conventional helicopter to navigate forward as its rotor disk size increases.

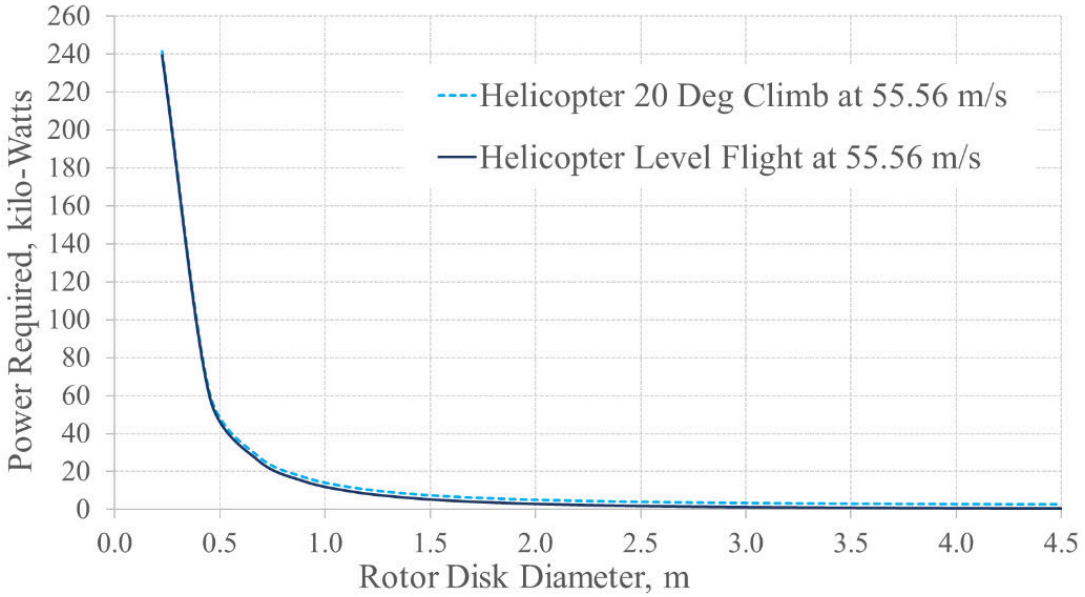

Figure 10. Forward Flight Power Required (at 55.56 m/s) vs Rotor Disk Diameter - 20 kg Martian Conventional Helicopter

The graph depicts how ascending during forward flight requires more power compared to level flight. However, for smaller rotor disk diameters, the power consumption for both flight modes remain similar, with the disparity between the two requirements becoming noticeable only at rotor disk diameters exceeding approximately 0.5 m. As the rotor disk size increases, the reduction in power requirements for forward climb flight is not as significant as that for level flight.

Figure 11 provides an overview of the power demands for forward level flight across all selected rotorcraft types, considering rotor disk diameters up to 9 m. Notably, at the smallest rotor disk size, conventional helicopters exhibit the highest and most excessive power requirement, followed by coaxial rotorcraft, tandem rotorcraft cases, two isolated rotors, quadcopter and finally hexacopter configurations. However, with a modest increase in rotor disk size, the power demand decreases rapidly, reaching a point where the difference in power becomes negligible beyond a rotor size of 2 m forward.

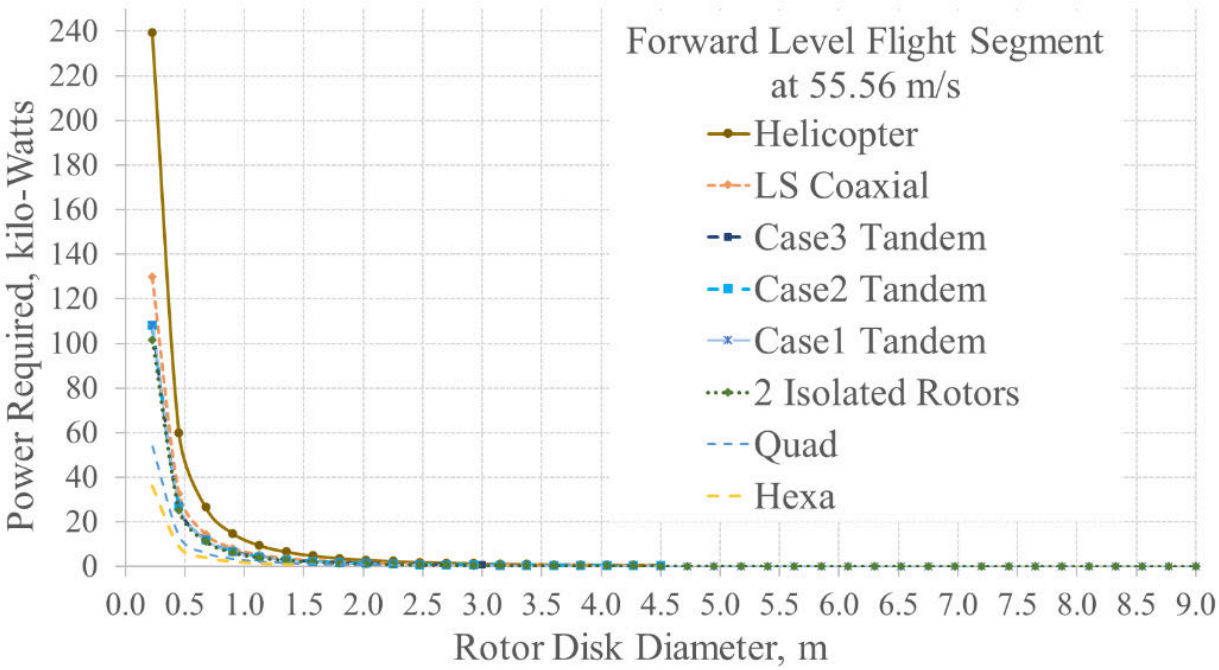

Figure 11 Forward Level Flight Power Required (at 55.56 m/s) vs Rotor Disk Diameter - 20 kg Martian Various Rotorcraft Configurations

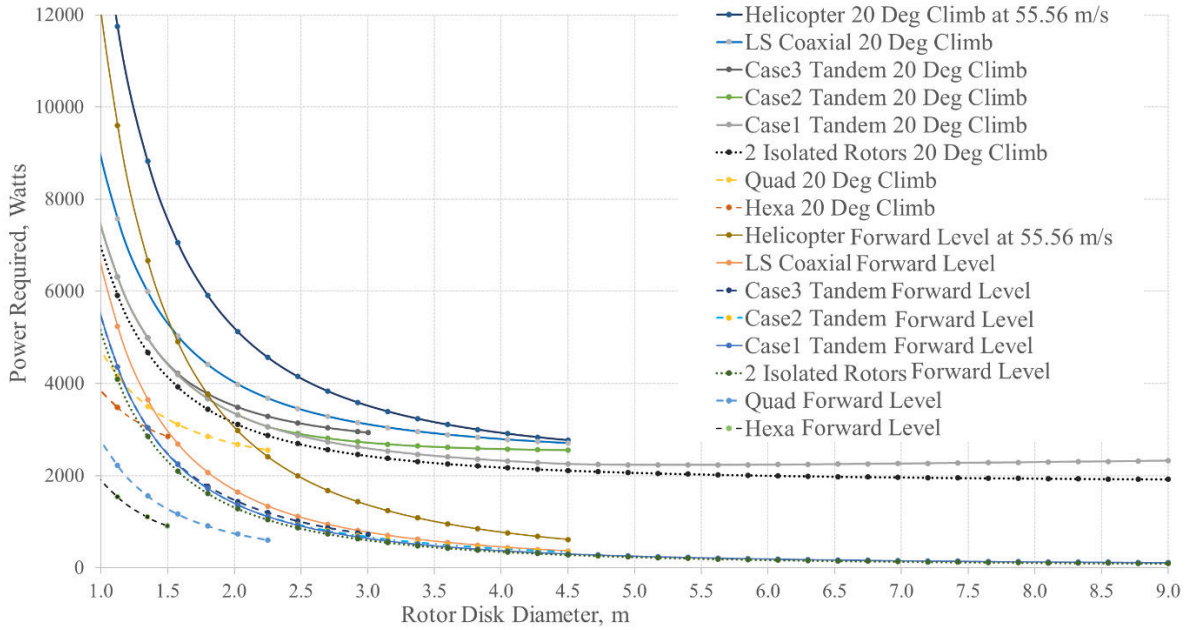

Figure 12. Forward Flight Power Required (at 55.56 m/s) vs Rotor Disk Diameter (Rotor Diameter Limits – 1 m to 9m) – Comparison between various 20 kg rotorcraft configurations (Helicopter, Coaxial, Tandem Cases, 2 Isolated Rotors, Quadcopter, Hexacopter)

Figure 12 zooms in on the power variations for forward level and climb flights across different rotorcraft configurations, with a rotor disk diameter starting from 1 m on the horizontal axis. An intriguing observation is noted in the forward climb of tandem rotorcraft Case 1, where power requirements surpass a minimum value at a specific overlapping rotor disk size. This increase occurs when the tandem rotors overlap, evident beyond a rotor diameter of 4.5 m for Case 1, due to the additional overlapping interference factor (K_{ov}) combined with the downwash factor (K_{dw}). Similarly, Case 2 of tandem rotorcraft exhibits a comparable pattern, albeit closer to the upper limit of the rotor diameter.

While climbing during forward flight necessitates more power than level flight, ascending while moving forward proves to be more energy efficient. Flying at a lower altitude reduces energy losses by creating an air cushion beneath the aircraft, known as ground effects, facilitating the attainment of optimal flying speed before ascent. To prevent the formation of air shocks at the rotor tip speed, this analysis is conducted at the maximum allowable forward flying speed. Experimenting with higher forward speeds could potentially reduce the required power. Similarly, reducing the climb path angle would lead to a decrease in the power required for forward climb flight.

6.3 BMF Comparative Analysis of Rotor Configurations

The Battery Mass Fraction (BMF) is depicted in Figure 13 by plotting the power required for vertical climb against the increasing rotor disk diameter for each designated rotorcraft configuration. In the calculation of BMF using Eq. (10), parameters such as a 2-minute run time (E), an 8.33 m/s climb speed, and a constant total mass of 20 kg are considered. The trend of the vertical climb BMF lines mirrors the dependency observed in Figure 9, where increasing power demands result in higher BMF values, indicating the necessary battery weight for this flight segment. Similarly, Figure 14 illustrates a comparable BMF trend for the forward leveled flight segments, reflecting the power requirements of the forward leveled flight shown in Figure 10.

The battery mass can be obtained by multiplying the BMF by the overall mass of the aircraft. For instance, a BMF of 0.05 would yield a battery mass of 1 kg (0.05 x 20 kg). It is important to note that the BMF for each segment needs to be combined with the BMF of other flight segments, as discussed in the third section, to determine the total BMF and the overall battery mass required for a specific flight regime. Additionally, it should be remembered that the BMF calculated for the flying mission does not include the battery mass needed for avionics and electronic payload instrumentation, which would require separate computations unless they are powered by independent batteries.

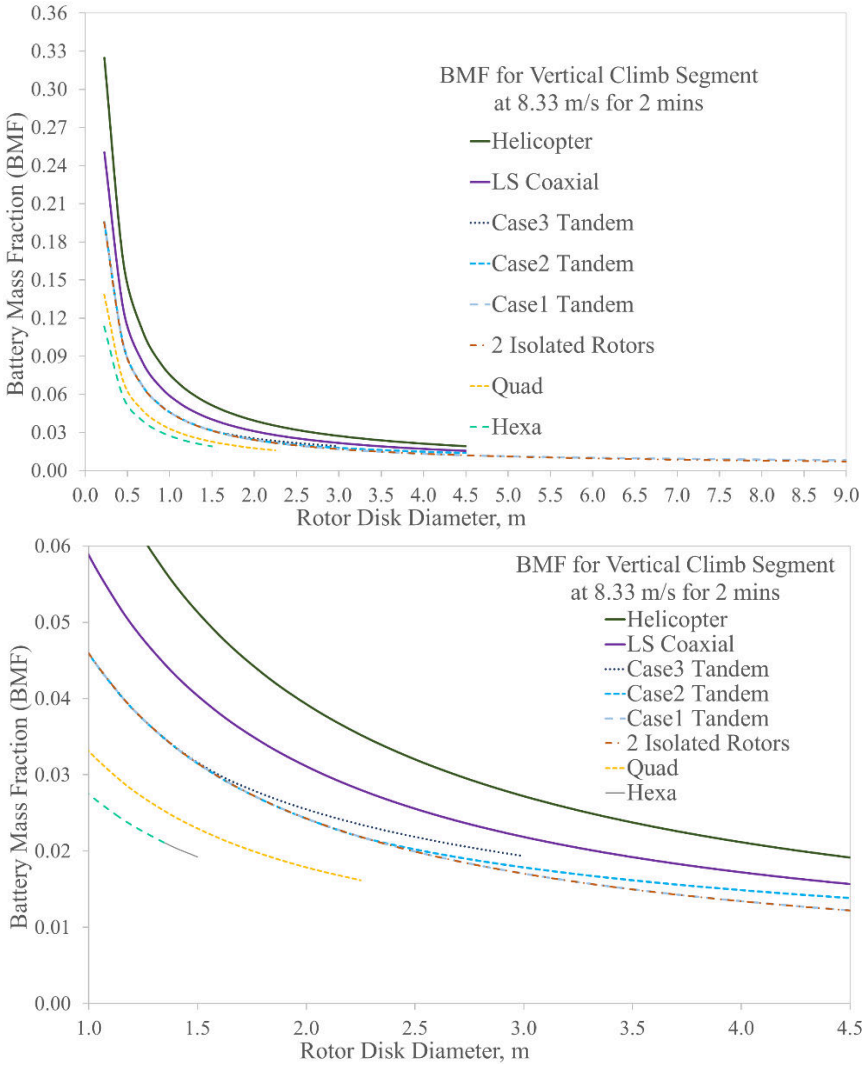

Figure 13. Vertical Climb (at 8.33 m/s for 2 mins) BMF vs Rotor Disk Diameter - 20 kg Martian rotorcrafts. Top - BMF for rotor diameters from 0 to 9 m. Bottom – Close-up view, focusing on BMF for rotor diameters from 1 m to 4.5 m on the x-axis for clarity

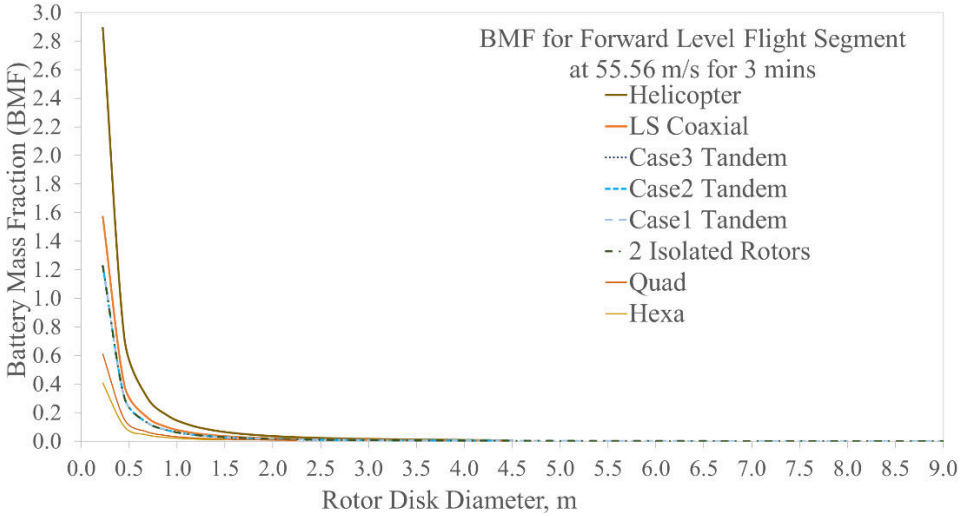

Figure 14. Forward Levelled Flight (at 55.56 m/s for 3 mins) BMF vs Rotor Disk Diameter - 20 kg Martian rotorcrafts

7. Discussion

In designing robots for extraterrestrial applications, simplicity is paramount to minimize the risk of malfunction, as physical maintenance or mechanical repairs may not be feasible. Selecting the most power-efficient rotorcraft configurations for aerobot design involves analyzing the power demands of

rotorcraft with single, dual, and multi rotors. For instance, considering the Case 1 Tandem rotorcraft with a 9 m rotor diameter, specific design constraints are implemented to exclude certain theoretical findings that, while theoretically optimal, introduce complexities. These constraints include the need for heavy and robust materials, folding and stowing requirements, as well as control and stability concerns. Similarly, smaller rotors are better suited for small to medium-sized multicopters and are advantageous only when they are lighter and mechanically simpler. Otherwise, incorporating more motors and hub systems increases the aircraft's empty weight and reduces payload capacity.

7.1 Power Efficient Rotor Configuration

Figure 15 and Figure 16 depict analytical graphs illustrating the power required by various rotorcraft configurations, including the conventional helicopter, LS (Large Separation) coaxial rotorcraft, three tandem rotorcraft cases, quadcopter, and hexacopter for vertical climb and forward level flight, respectively, in relation to the rotor disk diameter. The data depicted in these graphs highlight that, within the specified parameters, hexarotor configurations demand the least power compared to rotorcrafts with single and dual rotors, particularly for rotor sizes up to 1.5 m. According to the formulas utilised in this simplified approach, quadrotor and hexarotor operate as independent entities without overlapping interference, except for the downwash generated by frontal rotors during forward flight. This downwash effect can be minimized for quadrotor, thus enhancing power efficiency, by altering the quad setting from square to diamond [20]. When comparing power requirements between single and dual rotors, tandem rotorcraft displays the lowest power consumption. However, among the three tandem rotorcraft cases, Tandem Case 3 emerges as a priority, as outlined in [16], due to its comparatively simpler and lighter configuration, coupled with enhanced power efficiency.

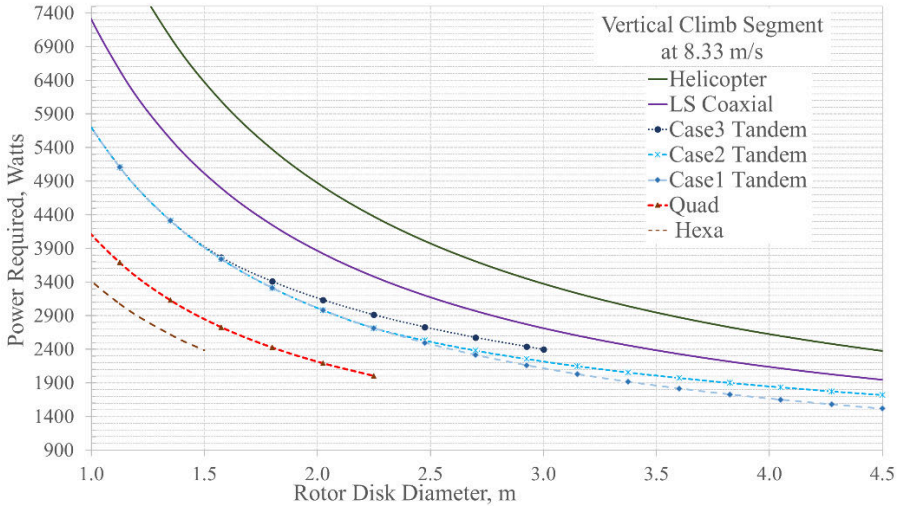

Figure 15. Power Required (Vertical Climb at 8.33 m/s) vs Rotor Disk Diameter (Rotor Diameter Limits – 1 m to 4.5m) – Comparison between various 20 kg rotorcraft configurations

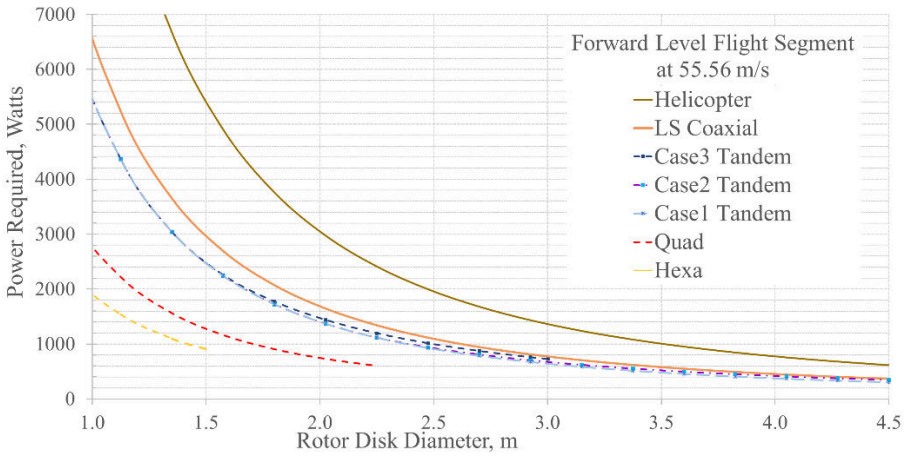

Figure 16. Power Required (Forward Level at 55.56 m/s) vs Rotor Disk Diameter (Rotor Diameter Limits – 1 m to 4.5m) – Comparison between various 20 kg rotorcraft configurations

7.2 Implementing Initial Sizing on Selected Configuration

A hexacopter configuration with a 1.5 m rotor disk size is selected for the initial sizing process. The power required for the vertical climb segment is determined to be 2386 Watts, while for the cruise segment, it is 909 Watts. The corresponding Battery Mass Fraction (BMF) values are calculated to be 0.019 and 0.01, respectively. Summing up these BMF values yields a total BMF of 0.029. Given the predetermined total aerobot mass of 20 kg, Eq. (10) is utilised to calculate the required battery mass (m_{b}) for the 5-minute flight mission, resulting in 0.58 kg. Additionally, considering that the aerobot must accommodate a science payload weighing 2 kg, Eq. (11) is used in terms of Mass to determine the available aircraft's empty mass, resulting in 17.42 kg. This represents 87.1% of the total aircraft mass, offering a feasible starting point for further analysis. The empty mass encompasses the rotorcraft's materials and components, which, for initial estimation purposes, can be sourced from Commercially Off-The-Shelf (COTS) components or similar aircraft. Through an iterative process, adjustments to the mass components can be made to achieve a more refined rotorcraft sizing, initiating the preliminary design phase.

8. Conclusion

Rotorcraft operations on Mars have been proven feasible through the successful flight of NASA's Mars Helicopter. To advance Mars rotorcraft technology, future missions will rely on advanced approaches built upon this foundation. Addressing a critical research gap, this study describes its objectives and establishes essential parameters for a comprehensive analysis of 20 kg rotorcraft configurations, encompassing both single and multiple rotor designs. Employing simplified equations derived from helicopter momentum theory, the methodology is adapted and streamlined for each rotorcraft configuration under examination. Furthermore, the study introduces an initial methodology for sizing battery-electric aircraft, utilizing the Battery Mass Fraction to estimate battery mass for different flight segments. Graphical representations depict the power requirements for hover, vertical ascent, and forward flight, correlating with increasing rotor disk diameter across various rotorcraft types, including conventional helicopters, coaxial rotorcraft, tandem rotorcraft, quadcopter and hexacopter. Notably, conventional helicopters exhibit higher power consumption than alternative configurations under the specified parameters. Rotorcraft with two isolated rotors is identified as advantageous due to their reduced aerodynamic interference caused by rotor overlap. Among multicopter configurations, hexacopters demonstrate superior performance, especially for rotor disk sizes up to 1.5 m. However, as rotor disk diameter approaches the upper limit, discrepancies in power requirements between configurations become marginal.

9. Contact Author Email Address

Vishal Youhanna Vishal.Youhanna@cranfield.ac.uk
Leonard Felicetti Leonard.Felicetti@cranfield.ac.uk
Dmitry Ignatyev D.Ignatyev@cranfield.ac.uk

10. Copyright Statement

The authors confirm that they, and/or their company or organization, hold copyright on all of the original material included in this paper. The authors also confirm that they have obtained permission, from the copyright holder of any third-party material included in this paper, to publish it as part of their paper. The authors confirm that they give permission, or have obtained permission from the copyright holder of this paper, for the publication and distribution of this paper as part of the ICAS proceedings or as individual off-prints from the proceedings.

References

[1] Hassanalian, M., Rice, D., & Abdelkefi, A. Evolution of space drones for planetary exploration: A review. *Progress in Aerospace Sciences*, 97, 2018. 61–105. https://doi.org/10.1016/J.PAEROSCI.2018.01.003

[2] NASA. Overview | Mars – *NASA Solar System Exploration*. Retrieved April 22, 2024, from https://solarsystem.nasa.gov/planets/mars/overview/

[3] Radotich, M., Withrow-Maser, S., deSouza, Z., Gelhar, S., & Gallagher, H. (2021, January). A study of past, present, and future Mars rotorcraft. In 9th Biennial Autonomous VTOL Technical Meeting.

[4] Johnson, W., Withrow-Maser, S., Young, L., Malpica, C., Koning, W. J. F., Kuang, W., Fehler, M., Tuano, A., Chan, A., Datta, A., Chi, C., Lumba, R., Escobar, D., Balaram, J., Tzanetos, T., & Fjaer Grip, H. (2020). Mars Science Helicopter Conceptual Design. http://www.sti.nasa.gov

[5] NASA. (2023) Mars Helicopter - *NASA Mars*. Retrieved April 22, 2024, from https://mars.nasa.gov/technology/helicopter/#Flight-Log

[6] Young, L. A., Chen, R. T. N., Aiken, E. W., Briggs, G. A., "Design Opportunities and Challenges in the Development of Vertical Lift Planetary Aerial Vehicles," Proceedings of the American Helicopter Society International Vertical Lift Aircraft Design Specialist's Meeting, January 2000.

[7] Underwood, C., & Collins, N. (2017). Design and Control of a Y-4 Tilt-Rotor VTOL Aerobot for Flight on Mars. Proceedings of the 68th International Astronautical Congress (IAC), 25–29. https://openresearch.surrey.ac.uk/esploro/outputs/conferencePresentation/Design-and-Control-of-a-Y-4-Tilt-Rotor-VTOL-Aerobot-for-Flight-on-Mars/99511131102346

[8] Aguirre, J., Casado, V., Chamie, N., & Zha, G. (2007). Mars Intelligent Reconnaissance Aerial and Ground Explorer (MIRAGE) AIAA 2007-244, Reno, Nevada. https://doi.org/10.2514/6.2007-244

[9] Forshaw, J., & Lappas, V. (2012). Architecture and Systems Design of a Reusable Martian Twin Rotor Tailsitter. *Acta Astronautica*, 80(0), 166–180. https://doi.org/10.1016/J.ACTAASTRO.2012.05.008

[10] RM Zubrin. (2012). The Mars Gashopper. *Concepts and Approaches for Mars 2012*. June 12-14, 2012 in Houston, Texas. https://ui.adsabs.harvard.edu/abs/2012LPICo1679.4069Z/abstract

[11] Fathepure, M., Booker, A. L., Abouzahr, O., Wang, N., & Tikalsy, D. (2021). Design and Construction of an Inflatable-Winged VTOL Mars Electric Flyer. In AIAA AVIATION 2021 FORUM (p. 2578) https://doi.org/10.2514/6.2021-2578

[12] Youhanna V, Felicetti L & Ignatyev D (2024). Preliminary Investigation into Future Martian Multicopter Configurations. In: Vertical Flight Society's 80th Annual Forum & Technology Display, Montréal, Québec, Canada, May 7-9, 2024. https://doi.org/10.4050/F-0080-2024-1266

[13] D. Raymer. *Aircraft design: A conceptual approach*, 6. Ed., AIAA education series, Reston, Va., 2018, Chaps. 20.11, 21.3.

[14] Leishman, J. Gordon. *Principles of Helicopter Aerodynamics*, 2. Ed., United Kingdom, Cambridge University Press, 2006. Chaps. 2.15, 5.5.11.

[15] Johnson, W. *Rotorcraft Aeromechanics*. Cambridge University Press. 2013. Chaps. 4.6, 5.3. https://doi.org/10.1017/CBO9781139235655

[16] Youhanna V, Felicetti L & Ignatyev D (2023). Conceptual Design Study based on Defined Parameters for Next Generation Martian Rotorcrafts. In: IEEE Aeroconf 2024, Montana, US, 2-9 March 2024. DOI: https://doi.org/10.1109/AERO58975.2024.10521441

[17] NASA. (2023) Mars Fact Sheet. *NASA Goddard Space Flight Center*. Retrieved April 22, 2024, from https://nssdc.gsfc.nasa.gov/planetary/factsheet/marsfact.html

[18] Millour, E., Forget, F., Spiga, A., Pierron, T., Bierjon, A., Montabone, L., Vals, M., Lefèvre, F., Chaufray, J.-Y., Lopez-Valverde, M., Gonzalez-Galindo, F., Lewis, S., Read, P., Desjean, M.-C., and Cipriani, F. and the MCD Team: The Mars Climate Database (Version 6.1), Europlanet Science Congress 2022, Granada, Spain, 18–23 Sep 2022, EPSC2022-786, https://doi.org/10.5194/epsc2022-786

[19] Balaram, J., Aung, M. & Golombek, M.P. The Ingenuity Helicopter on the Perseverance Rover. *Space Sci Rev* 217, 56 (2021). https://doi.org/10.1007/s11214-021-00815-w

[20] Han, D., & Barakos, G. N. (2020). Aerodynamic interference model for multirotors in forward flight. *Journal of Aircraft*, 57(6), 1220–1223. https://doi.org/10.2514/1.C035978/ASSET/IMAGES/LARGE/FIGURE3.JPEG

https://dspace.org/

Preliminary design exploration of prospective multirotor aerobots

Youhanna, Vishal; Felicetti, Leonard; Ignatyev, Dmitry

2024-09-30
International Council of the Aeronautical Sciences (ICAS)
https://www.icas.org/icas_archive/icas2024/data/papers/icas2024_0536_paper.pdf
Youhanna V, Felicetti L, Ignatyev D. (2024) Preliminary design exploration of prospective multirotor aerobots. 34th Congress of the International Council of the Aeronautical Sciences (ICAS), 9-13 September 2024, Florence, Italy

Downloaded from a DSpace repository. https://dspace.org/